

Synthesis, Crystal Structure and Electrochemical Properties of a New Adduct of Benzo-15-crown-5 and $\text{H}_3\text{PMo}_{12}\text{O}_{40}$

Qinghua Du, Dawei Song, Wansheng You, Yi Zhao, Tingting Gan, and Limei Dai

Institute of Chemistry for Functionalized Materials, Liaoning Normal University, Dalian, Liaoning 116029, P. R. China

Reprint requests to Prof. Wangsheng You. Fax: 86-411-82156858. E-mail: wsyu@lnnu.edu.cn

Z. Naturforsch. **2009**, *64b*, 274–280; received November 5, 2008

A new crown ether-POM (POM = polyoxometalate) adduct with the molecular formula $[(\text{C}_{14}\text{H}_{20}\text{O}_5)_4(\text{H}_3\text{O})_3]\text{PMo}_{12}\text{O}_{40} \cdot 0.5\text{CH}_3\text{CN}$ (**1**) was isolated from the mixed solvent of acetonitrile and methanol. The adduct is constructed from Keggin $[\text{PMo}_{12}\text{O}_{40}]^{3-}$ anions and $[(\text{C}_{14}\text{H}_{20}\text{O}_5)(\text{H}_3\text{O}^+)]$ and $[(\text{C}_{14}\text{H}_{20}\text{O}_5)_2(\text{H}_3\text{O}^+)]$ cations *via* electrostatic and hydrogen bonding interactions. The supramolecular interactions combine the crown ether with oxonium ions. In the $[(\text{C}_{14}\text{H}_{20}\text{O}_5)(\text{H}_3\text{O}^+)]$ moieties, the oxonium ions reside out of the planes defined by the oxygen atoms of the crown ether. The $[(\text{C}_{14}\text{H}_{20}\text{O}_5)_2(\text{H}_3\text{O}^+)]$ moieties exhibit a sandwich structure. There exist hydrogen bonds between the oxonium ions of the $[(\text{C}_{14}\text{H}_{20}\text{O}_5)(\text{H}_3\text{O}^+)]^+$ cations and the acetonitrile molecules and the terminal and bridging oxygen atoms of the $[\text{PMo}_{12}\text{O}_{40}]^{3-}$ anions. The adduct has been used as a bulk-modifier to fabricate a chemically modified carbon paste electrode (MCPE), which displays well-defined cyclic voltammograms with three reversible two-electron redox couples in acidic aqueous solution, and electrocatalytic activities towards the reduction of H_2O_2 and NO_2^- .

Key words: Polyoxometalate, Benzo-15-crown-5, Adduct, Carbon Paste Electrode

Introduction

The adducts based on polyoxometalates and crown ethers have been applied in the membranes of Pb^{2+} -selective electrodes, which exhibit better sensitivities with lower detection limits and a wider linear detection concentration range [1]. In crown ether-POM adducts, the dominant interactions between $[\text{crown-M}]^+$ (M = metal ions [2–9] or oxonium ions [10–15]) cations and polyoxometalate anions are generally electrostatic interactions, but there also exist other supramolecular interactions [3, 6]. We prefer to use this term to describe the interactions between crown ether molecules and oxonium ions as some authors consider them as hydrogen bonds [14, 15], while others think they are predominantly electrostatic interactions [12]. Crown ether molecules can capture hydrated oxonium ions $([\text{H}(\text{H}_2\text{O})_n]^+, n = 1 \text{ to } ca. 20)$ [16–22] through these supramolecular interactions, and the oxonium ions can reside above the crown ether molecules [17–19] or are sandwiched by crown ether molecules [14, 15, 20–22]. Recently, Akutagawa *et al.* have reported a solid-state molecular rotator, $(\text{Cs}^+)_3([\text{18}]\text{crown-6})_3(\text{H}^+)_2[\text{PMo}_{12}\text{O}_{40}]^{5-}$, in which two Cs^+ ([18]crown-6) supramolecular rotators were

complexed with $[\text{PMo}_{12}\text{O}_{40}]^{5-}$ Keggin clusters [23]. To the best of our knowledge, hydrogen bonding interactions between crown ether-oxonium moieties and surface oxygen atoms of POMs have not been reported until now, unlike those in other adducts of crown ether-metal ions. Two significant features of crown ether-POM adducts merit attention. Firstly, the adducts are insoluble in aqueous solutions and secondly, crown ethers are electrochemically inert. These results have encouraged us to study carbon paste electrodes chemically modified with POMs [24]. In this paper, we report the supramolecular structure and electrochemical properties of a new crown ether-POM adduct, $[(\text{C}_{14}\text{H}_{20}\text{O}_5)_4(\text{H}_3\text{O})_3] \cdot [\text{PMo}_{12}\text{O}_{40}] \cdot 0.5\text{CH}_3\text{CN}$ (**1**).

Results and Discussions

Benzo-15-crown-5 and $\text{H}_3\text{PMo}_{12}\text{O}_{40} \cdot 24\text{H}_2\text{O}$ were dissolved at r.t. in a mixture of acetonitrile and methanol. Upon evaporation of the solvent mixture adduct **1** was formed and could be isolated.

IR spectrum

In the IR spectrum, the bands at 1061, 958, 881, 804 cm^{-1} are assigned to $\nu(\text{P}-\text{O}_c)$, $\nu(\text{Mo}=\text{O}_t)$,

$\nu(\text{Mo}-\text{O}_b-\text{Mo})$, and $\nu(\text{Mo}-\text{O}_c-\text{Mo})$, respectively, and those at 2916 and 2871 cm^{-1} are attributed to crown ether $-\text{CH}_2-$ groups. The peaks from 1594 to 1099 cm^{-1} indicate the stretching frequencies of the $-\text{C}-\text{O}-$ groups.

Crystal structure description

The crystal structure analysis has revealed that adduct **1** consists of one $[\text{PMo}_{12}\text{O}_{40}]^{3-}$ anion, one $[(\text{C}_{14}\text{H}_{20}\text{O}_5)_2(\text{H}_3\text{O}^+)]$ moiety, two $[(\text{C}_{14}\text{H}_{20}\text{O}_5)-(\text{H}_3\text{O}^+)]$ moieties and 0.5 acetonitrile molecule. The anion has a classical α -Keggin structure exhibiting T_d symmetry. The PO_4 tetrahedron is surrounded by twelve MoO_6 octahedral units arranged in four groups of three edge-sharing Mo_3O_{13} trinuclear units linked together by sharing corners. The bond lengths and bond angles, shown in Table 2, are in close agreement with those described in the literature [12, 15].

As shown in Fig. 1a, there exist three crystallographically independent water molecules, O1W, O2W, O3W, which are protonated to oxonium ions, H_3O^+ . The O1W and O2W ions reside out of the planes defined by the oxygen atoms of the corresponding crown ethers, and the distances between oxonium ions and the centers of the crown ether rings are 1.002(4) and 0.898(4) Å. The supramolecular interactions (filled dashed bonds in Fig. 1a) combine the crown ether with the oxonium ions. Each O3W ion is sandwiched between a pair of benzo-15-crown-5 molecules, which are almost parallel with a twist angle is 65° (Fig. 1b). It is obvious that the distances between the O3W oxonium ions and the crown ethers are longer than those of O1W and O2W.

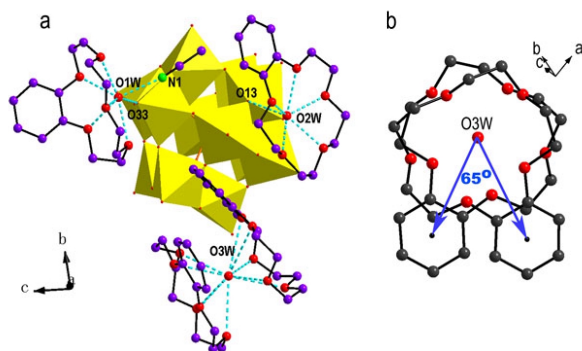


Fig. 1. a) Molecular structure of **1**, all H atoms are omitted (the filled dashed bonds are supramolecular interactions); b) the sandwich structure of $[(\text{C}_{14}\text{H}_{20}\text{O}_5)_2(\text{H}_3\text{O}^+)]$ moieties whose twist angle is 65° .

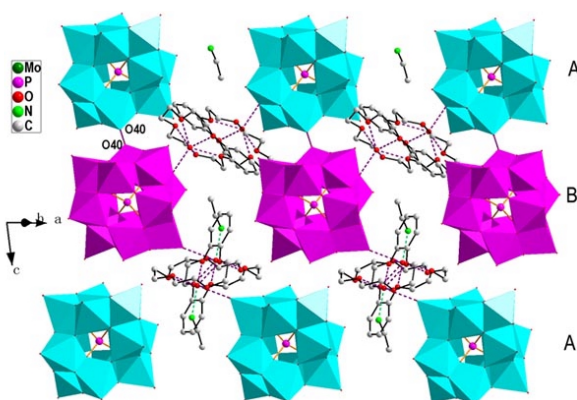


Fig. 2. Assemblage of $[\text{PMo}_{12}\text{O}_{40}]^{3-}$ polyoxoanions and $[(\text{C}_{14}\text{H}_{20}\text{O}_5)(\text{H}_3\text{O}^+)]$ cationic groups along the c axis.

There exist hydrogen bonding interactions between the O1W oxonium ion and the O33 atom of a $[\text{PMo}_{12}\text{O}_{40}]^{3-}$ anion (2.638(2) Å), the O1W oxonium ion and the N atom of a CH_3CN molecule (2.384(2) Å), and the O2W oxonium ion and the bridging O13 atom of a $[\text{PMo}_{12}\text{O}_{40}]^{3-}$ anion (2.827(2) Å). Through these interactions, a $[\text{PMo}_{12}\text{O}_{40}]^{3-}$ anion, an O1W oxonium ion, an O2W oxonium ion and a CH_3CN molecule constitute a basic unit. The units are packed in two opposite orientations, forming the $\text{AB}\cdots\text{AB}$ mode along the crystallographic c axis. The distance of the O40 atoms of the $[\text{PMo}_{12}\text{O}_{40}]^{3-}$ anions between layer A and layer B is 2.717(3) Å (Fig. 2). The short distance may result from the packing mode or from weak interactions between O atoms, and this phenomenon has already been reported in the literature [25].

Electrochemical behavior

Voltammetric behavior of **1**-MCPE in aqueous electrolyte

The cyclic voltammograms for **1**-MCPE in 0.2 M H_2SO_4 aqueous solution at different scan rates are presented in Fig. 3. Three reversible redox peaks appear in the potential range of -200 to 800 mV and with half-wave potentials $E_{1/2} = (E_{pa} + E_{pc})/2$ of 315, 173, and -62 mV, respectively. Redox peaks I-I', II-II' and III-III' can be attributed to three consecutive two-electron processes of the Mo atoms. The peak potentials change gradually following the scan rates, the cathodic peak potentials shift towards the negative direction and the corresponding anodic peak potentials to the positive direction with increasing scan rates. This common phenomenon results from the

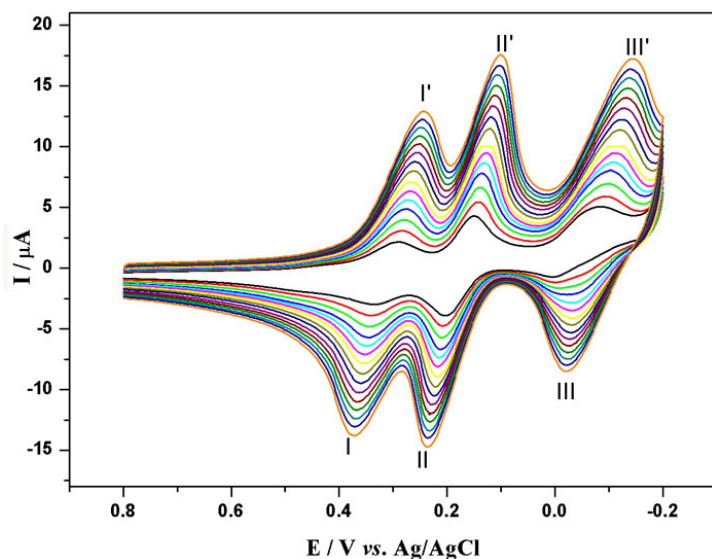


Fig. 3. Cyclic voltammograms of **1-MCPE** in 0.2 M H_2SO_4 at different scan rates (from inner to outer: 150, 200, 250, ... 800 mV s^{-1}).

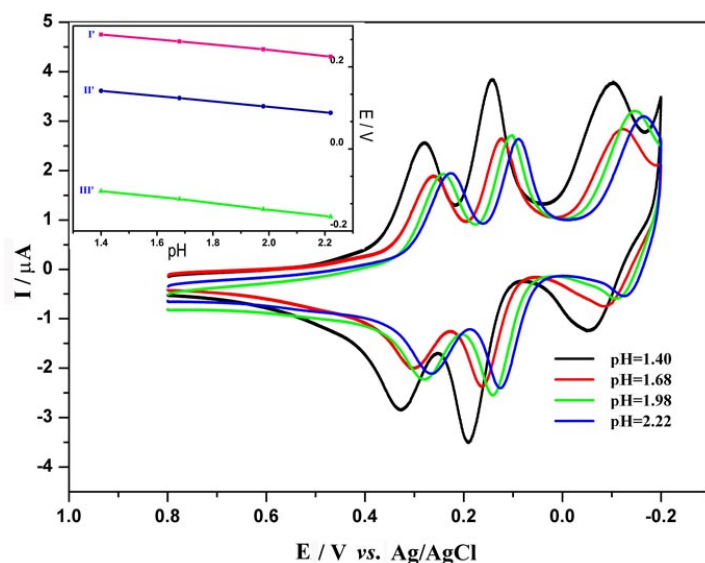


Fig. 4. Cyclic voltammograms of **1-MCPE** in H_2SO_4 solutions with different pH (from left to right: 1.40, 1.68, 1.98, 2.22). Inset: peak potentials plotted against pH value show linearity.

electron exchange rate between the electrode and the $[\text{PMo}_{12}\text{O}_{40}]^{3-}$ anions.

pH-Dependent electrochemical behavior of 1-MCPE

Fig. 4 shows cyclic voltammograms for **1-MCPE** in acidic aqueous solutions at different pH. It can be clearly seen that the three waves shift to more negative potentials with increasing pH value. Plots of peak potentials of three cathodic waves *versus* pH for the **1-MCPE** show linearity in the pH range from 1.40 to 2.22 (three curves in the inset), and the slopes of

the pH range are 65.8, 65.4 and 76.8 mV/pH for the three reduction peaks, respectively, approximately corresponding to the addition of two protons, as was observed with solution phase and multifold species of $\text{PMo}_{12}\text{O}_{40}^{3-}$ [26, 27].

Electrocatalytic reduction of H_2O_2 and NO_2^- on 1-MCPE

The reduction of hydrogen peroxide at a bare electrode generally requires a large overpotential, and no obvious response is observed in the range +600

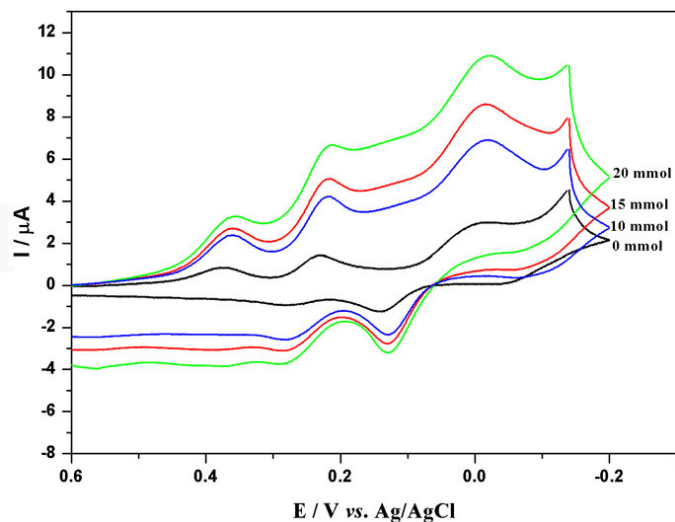


Fig. 5. **1**-MCPE's electrocatalytic activity toward the reduction of H₂O₂ in 0.2 M H₂SO₄ solution. Scan rate: 40 mV s⁻¹.

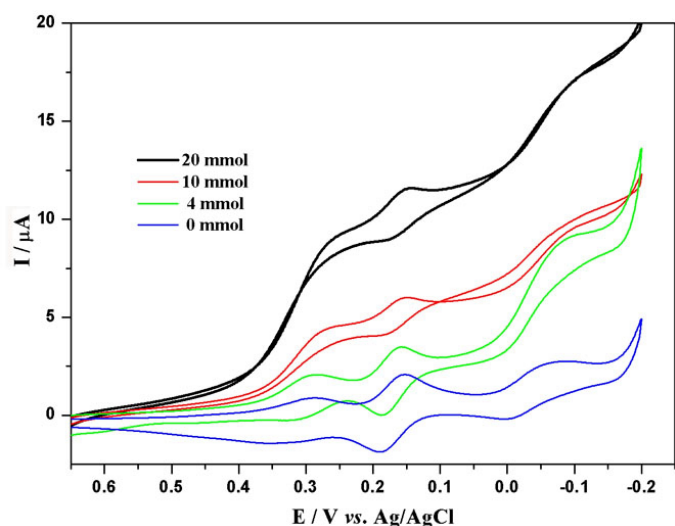


Fig. 6. **1**-MCPE's electrocatalytic activity toward NaNO₂ in 0.2 M H₂SO₄ solution. Scan rate: 40 mV s⁻¹.

to -150 mV [28]. **1**-MCPE displays electrocatalytic activity toward the reduction of H₂O₂. As shown in Fig. 5, the reduction peak currents increase, and the corresponding oxidation peak currents decrease with the increase in concentration of H₂O₂. The result indicates that the three reduced species of the [PMo₁₂O₄₀]³⁻ anions have electrocatalytic activity for H₂O₂ reduction.

Analogously, the three reduction peak currents increase, while the corresponding oxidation peak currents decrease, with the addition of NO₂⁻ at the **1**-MCP (Fig. 6). These results suggest that the three reduced species of the [PMo₁₂O₄₀]³⁻ anions have electrocatalytic activity for NO₂⁻ reduction.

Stability of **1**-MCPE

When the potential range is maintained at -200 to 800 mV, the electrode is stable over 300 cycles at a rate of 100 mV s⁻¹, and the peak currents only decrease by less than 5%. After storage at r.t. for 20 d, the peak currents remain almost unchanged. The remarkable stability of the modified electrodes can be attributed to the insolubility of the crown ether-POM supramolecular assemblies and the affinity of the crown ethers toward the paste.

Thermal analysis

The thermal analysis of **1** gives a weight loss of 2.6% in the range of 90–130 °C, which is corre-

Table 1. Crystal data and structure refinement for adduct **1**.

Formula	C ₅₇ H _{81.5} Mo ₁₂ N _{0.5} O ₆₃ P
Formula weight	2963.98
Crystal size, mm ³	0.30 × 0.30 × 0.10
Crystal system	triclinic
Space group	<i>P</i> $\bar{1}$
<i>a</i> , Å	14.671(2)
<i>b</i> , Å	16.566(2)
<i>c</i> , Å	19.677(3)
α , deg	84.208(2)
β , deg	83.508(2)
γ , deg	78.295(2)
<i>V</i> , Å ³	4638.1(11)
<i>Z</i>	2
<i>D</i> _{calcd} , g cm ⁻³	2.122
μ (MoK α), mm ⁻¹	1.689
<i>F</i> (000), e	2900
<i>hkl</i> range	-17 ≤ <i>h</i> ≤ +17, -19 ≤ <i>k</i> ≤ +16, -23 ≤ <i>l</i> ≤ +18
Refl. measured / unique / <i>R</i> _{int}	23493 / 16130 / 0.0312
Param. refined	1216
<i>R</i> 1/ <i>wR</i> 2 ^a [<i>I</i> ≥ 2 σ (<i>I</i>)]	0.0586/0.1436
<i>R</i> 1/ <i>wR</i> 2 ^a (all data)	0.1045/0.1637
GoF (<i>F</i> ²) ^a	1.038
$\Delta\rho_{\text{fin}}$ (max / min), e Å ⁻³	1.32 / -1.46

^a $R1 = \frac{\sum |F_o| - |F_c|}{\sum |F_o|}$, $wR2 = \frac{[\sum w(F_o^2 - F_c^2)^2 / \sum w(F_o^2)^2]^{1/2}}{w}$, $w = \frac{1}{[\sigma^2(F_o^2) + (0.0733P)^2 + 2.2123P]^{-1}}$, where $P = \frac{(\text{Max}(F_o^2, 0) + 2F_c^2)}{3}$; $GoF = \frac{[\sum w(F_o^2 - F_c^2)^2 / (n_{\text{obs}} - n_{\text{param}})]^{1/2}}$.

sponding to the loss of the acetonitrile and coordinated water (calcd. 2.5 %). The second weight loss from 235 to 530 °C is ascribed to the benzo-15-crown-5 decomposition (showing a weight loss of 36.5 %; the calculated value is 36.2 %).

Conclusion

In summary, a new crown ether-POM adduct, [(C₁₄H₂₀O₅)₄(H₃O)₃][PMo₁₂O₄₀] · 0.5 CH₃CN (**1**), has been synthesized and applied in chemically modified carbon paste electrodes. Adduct **1** is constructed from [PMo₁₂O₄₀]³⁻ anions, [(C₁₄H₂₀O₅)(H₃O⁺)] cations, and sandwich [(C₁₄H₂₀O₅)₂(H₃O⁺)] cations. Through supramolecular interactions, a [PMo₁₂O₄₀]³⁻ anion, two oxonium ions and one CH₃CN molecule constitute a basic unit. The units are packed in two opposite orientations, resulting in the sequence AB...AB along the crystallographic *c* axis. This is an excellent example of a packing mode resulting from supramolecular interactions in inorganic-organic hybrids. **1**-MCPE displays well-defined cyclic voltammograms with three reversible two-electron redox couples in acidic aqueous solution, exhibits electrocatalytic activities toward the reduction of H₂O₂

Table 2. Selected bond lengths (Å) and angles (deg) for adduct **1**.

Mo(1)–O(5)	1.660(6)	O(2W)–O(55)	2.376(18)
Mo(1)–O(2)	1.835(6)	O(3W)–O(46)	3.121(18)
Mo(1)–O(1)	1.867(5)	O(3W)–O(47)	2.909(18)
Mo(1)–O(3)	1.966(6)	O(3W)–O(48)	2.864(18)
Mo(1)–O(4)	1.996(6)	O(3W)–O(49)	2.932(18)
Mo(1)–O(38)	2.442(5)	O(3W)–O(50)	3.043(18)
P(1)–O(39)	1.522(6)	O(3W)–O(56)	2.986(18)
P(1)–O(37)	1.532(5)	O(3W)–O(57)	2.979(18)
P(1)–O(38)	1.539(6)	O(3W)–O(58)	2.909(18)
P(1)–O(15)	1.543(6)	O(3W)–O(59)	2.908(18)
O(41)–C(7)	1.440(11)	O(3W)–O(60)	3.173(18)
O(41)–C(5)	1.353(12)		
O(42)–C(9)	1.419(12)	O(5)–Mo(1)–O(2)	104.0(3)
O(42)–C(8)	1.420(13)	O(5)–Mo(1)–O(1)	102.4(3)
O(43)–C(11)	1.411(13)	O(2)–Mo(1)–O(1)	95.8(2)
O(43)–C(10)	1.427(13)	O(8)–Mo(2)–O(3)	104.1(3)
O(44)–C(13)	1.305(17)	O(8)–Mo(2)–O(9)	102.3(3)
O(44)–C(12)	1.404(14)	O(3)–Mo(2)–O(9)	94.2(3)
O(45)–C(1)	1.342(13)	O(8)–Mo(2)–O(7)	101.6(3)
O(45)–C(14)	1.457(18)	O(3)–Mo(2)–O(7)	85.1(2)
O(1W)–N(1)	2.384(18)	O(14)–Mo(3)–O(11)	102.4(3)
O(1W)–O(33)	2.638(18)	O(14)–Mo(3)–O(10)	102.8(3)
O(1W)–O(41)	2.425(18)	O(11)–Mo(3)–O(10)	95.2(3)
O(1W)–O(42)	2.439(18)	O(14)–Mo(3)–O(13)	100.5(3)
O(1W)–O(43)	2.423(18)	O(11)–Mo(3)–O(13)	155.8(3)
O(1W)–O(44)	2.460(18)	O(27)–Mo(8)–O(26)	103.7(3)
O(1W)–O(45)	2.445(18)	O(27)–Mo(8)–O(6)	101.5(3)
O(2W)–O(13)	2.827(18)	O(6)–Mo(8)–O(24)	156.1(3)
O(2W)–O(51)	2.431(18)	O(30)–Mo(9)–O(20)	102.4(3)
O(2W)–O(52)	2.389(18)	O(20)–Mo(9)–O(23)	86.1(2)
O(2W)–O(53)	2.400(18)	O(35)–Mo(10)–O(37)	85.4(2)
O(2W)–O(54)	2.450(18)	O(9)–Mo(10)–O(37)	71.4(2)

and NO₂⁻, and shows excellent stability due to the insolubility of the crown ether-POM adducts.

Experimental Section

Materials and methods

All chemicals purchased were of reagent grade and used without further purification. H₃PMo₁₂O₄₀ · 24H₂O was synthesized according to the literature [29]. Elemental analysis (C, H and N) was performed on a Perkin-Elmer 2400 CHN Elemental Analyzer. Infrared spectra were recorded from KBr pellets on a TENSOR27 Bruker AXS spectrometer. The TG/DTA analysis was performed on a Pyris Diamond TG/DTA instrument in flowing air with a heating rate of 10 °C min⁻¹. The XPS measurement of Mo was carried out on a VG ESCALABMK spectrometer with an MgK α (1253.6 eV) achromatic X-ray source. The modified carbon paste electrode (MCPE) was fabricated as follows: 0.1 g graphite powder (purchased from Shanghai Chemical Plant and used as received) and 30 mg of adduct **1** were

mixed and ground together in an agate mortar to achieve a uniform and dry mixture. Paraffin (0.3 mL) was added to the mixture and stirred with a glass rod, then the homogenized mixture was used to pack 3 mm inner diameter quartz tubes. The surface was wiped with paper, and the electrical contact was established with a copper rod through the back of the quartz tubes. All electrochemical measurements were carried out on a CHI 600B electrochemical workstation at r. t. under nitrogen atmosphere. The working electrode was the 1-MCPE. A platinum wire was used as the counter electrode, and Ag/AgCl (3 M KCl) was the reference electrode.

Synthesis

A 10 mL acetonitrile solution of benzo-15-crown-5 (0.065 g, 0.24 mmol) was added to a 40 mL methanol solution of 0.7 g H₃PMo₁₂O₄₀ · 24H₂O (0.35 mmol) and 0.2 g La(NO₃)₃ · 6H₂O with stirring at r. t. The filtrate from this reaction mixture was allowed to stand for several days. Black crystals of adduct **1** (0.12 g) were collected. Yield: 67 % based on benzo-15-crown-5. Anal. calcd. (found): C 23.03 (23.11), H 3.07 (3.17), O 33.90 (33.95), N 0.24 (0.21), P 1.04 (1.02), Mo 38.72 (38.45)%.

Single crystal X-ray diffraction

Intensity data were collected on a SMART APEX II-CCD X-ray single crystal diffractometer at 293 K using graphite-monochromatized MoK_α radiation ($\lambda = 0.71073 \text{ \AA}$). An empirical absorption correction was applied. The structure was solved by Direct Methods and refined by full-matrix least-squares on F^2 using the SHELX-97 software package [30]. All non-hydrogen atoms were refined anisotropically, and the hydrogen atoms attached to carbon atoms were added in idealized geometrical positions. 78 restraints were applied to the fixed distances of the C–C bonds and to the isotropic refinements of some atoms of benzo-15-crown-5 and CH₃CN molecules. Some relevant crystallographic data and structure determination parameters are summarized in Table 1. Selected bond lengths and bond angles of **1** are listed in Table 2.

CCDC-700747 contains the supplementary crystallographic data for this paper. Copies of the data can be obtained free of charge from the Cambridge Crystallographic Data Centre via www.ccdc.cam.ac.uk/data_request/cif.

Acknowledgement

This work was financially supported by the National Natural Science Foundation of China (Grant No. 20773057) and the Liaoning Provincial Educational Commission (project No. 605L207).

-
- [1] S. Sheem, J. Shin, *Analyst*. **1992**, *117*, 1691–1695.
[2] V. Shivaiah, *Inorg. Chem. Commun.* **2006**, *9*, 1191–1194.
[3] W. S. You, E. B. Wang, Y. Xu, Y. G. Li, L. Xu, C. W. Hu, *Inorg. Chem.* **2001**, *40*, 5468–5471.
[4] V. Shivaiah, S. K. Das, *Angew. Chem.* **2006**, *118*, 251–254; *Angew. Chem. Int. Ed.* **2006**, *45*, 245–248.
[5] V. Shivaiah, S. K. Das, *Inorg. Chem.* **2005**, *44*, 7313–7315.
[6] X. M. Lu, B. Liu, Sarula, J. Wang, C. H. Ye, *Polyhedron* **2005**, *24*, 2889–2893.
[7] X. M. Lu, R. Zhong, S. C. Liu, Y. Liu, *Polyhedron* **1997**, *16*, 3865–3872.
[8] P. C. Junk, B. Moubarak, K. S. Murray, *Polyhedron* **2007**, *26*, 237–243.
[9] Y. G. Li, N. Hao, E. B. Wang, M. Yuan, C. W. Hu, N. H. Hu, H. Q. Jia, *Inorg. Chem.* **2003**, *42*, 2729–2735.
[10] X. M. Lu, H. J. Zhu, S. C. Liu, *Chin. Chem. Lett.* **1994**, *5*, 67.
[11] W. S. You, E. B. Wang, H. Zhng, L. Xu, Y. B. Wang, *J. Mol. Struct.* **2000**, *554*, 141–147.
[12] W. S. You, E. B. Wang, L. Xu, Z. M. Zhu, Y. P. Gu, *J. Mol. Struct.* **2002**, *605*, 41–49.
[13] W. S. You, E. B. Wang, Q. L. He, L. Xu, *J. Mol. Struct.* **2000**, *524*, 133–139.
[14] F. A. A. Paz, F. L. Soula, A. M. V. Cavaleiro, J. Kiliowski, T. Trindade, *Acta. Crystallogr.* **2004**, *E60*, m1–m5.
[15] P. C. R. Soares-Santos, L. Cunha-Silva, F. L. Sousa, L. M. J. Rocha, A. M. V. Cavaleiro, T. Trindade, F. A. A. Paz, J. Klinowski, H. I. S. Nrgueira, *J. Mol. Struct.* **2008**, *888*, 99–106.
[16] D. Braga, M. Gandolfi, M. Lusi, M. Polito, K. Rubini, F. Grepioni, *Cryst. Growth Des.* **2007**, *7*, 919–924.
[17] J. L. Atwood, P. C. Junk, *J. Chem. Soc., Dalton Trans.* **1997**, 4393–4400.
[18] H. Hassaballa, J. W. Steed, P. C. Junk, M. R. J. Elsegood, *Inorg. Chem.* **1998**, *37*, 4666–4671.
[19] J. L. Atwood, S. G. Bott, P. C. Junk, M. T. May, *J. Organomet. Chem.* **1995**, *487*, 7–15.
[20] R. D. Rogers, A. H. Bond, W. G. Hipple, A. N. Rollina, R. F. Henry, *Inorg. Chem.* **1991**, *30*, 2671–2679.
[21] D. Steinborn, O. Gravenhorst, H. Hartung, U. Baumeister, *Inorg. Chem.* **1997**, *36*, 2195–2199.
[22] M. Calleja, K. Johnson, W. J. Belcher, J. W. Steed, *Inorg. Chem.* **2001**, *40*, 4978–4985.
[23] T. Akutagawa, D. Endo, F. Kudo, S. Noro, S. Takeda, L. Cronin, T. Nakamura, *Cryst. Growth. Des.* **2008**, *8*, 812–816.
[24] D. W. Song, W. S. You, Y. Z. T. H. Hu, Q. H. Du, X. F. Zheng, *J. Mol. Struct.* **2008**, *888*, 337–343.

- [25] M. H. Alizadeh, M. Mirzaei, H. Razavi, *Mater. Res. Bull.* **2008**, *43*, 546–555.
- [26] N. Fay, E. Dempsey, T. McComac, *J. Electroanal. Chem.* **2005**, *574*, 359–366.
- [27] S. Y. Zhai, S. Y. Gong, J. G. Jiang, S. J. Dong, J. H. Li, *Anal. Chim. Acta* **2003**, *486*, 85–92.
- [28] X. L. Wang, Z. H. Kang, E. Wang, C. Hu, *J. Electroanal. Chem.* **2002**, *523*, 142–149.
- [29] X. Wu, *J. Biol. Chem.* **1929**, *18*, 43.
- [30] G. M. Sheldrick, SHELXS/L-97, Programs for Crystal Structure Determination, University of Göttingen, Göttingen (Germany) **1997**; see also: G. M. Sheldrick, *Acta Crystallogr.* **2008**, *A64*, 112–122.